Supporting Information

Hydrogen Bonding in the Active Site of Ketosteroid Isomerase:

Electronic Inductive Effects and Hydrogen Bond Coupling

Philip Hanoian,[‡] Paul A. Sigala,[§] Daniel Herschlag,[§] and Sharon Hammes-Schiffer*[‡]

Department of Chemistry, 104 Chemistry Building, Pennsylvania State University, University Park, Pennsylvania 16802, and Department of Biochemistry, Stanford University, Stanford, California 94305-5080
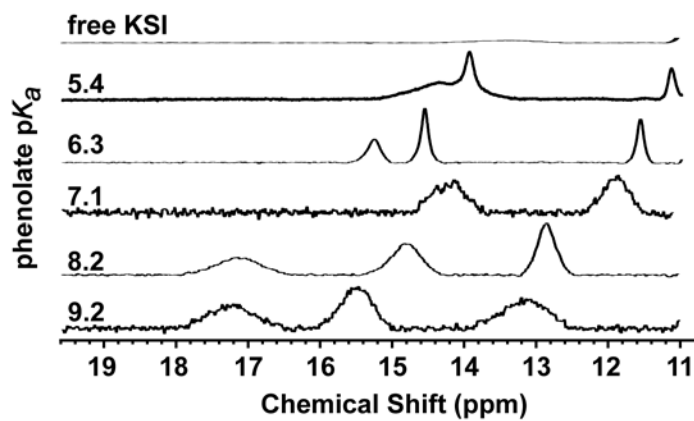
Figure S1: Downfield region of ^{1}H NMR spectra for substituted phenolates bound to pKSI D40N. The phenolates (pK$_a$) shown are 3,4-dinitrophenol (5.4), 3-trifluoromethyl-4-nitrophenol (6.3), 4-nitrophenol (7.1), 3-fluoro-5-trifluoromethylphenol (8.2), and 3-iodophenol (9.2).
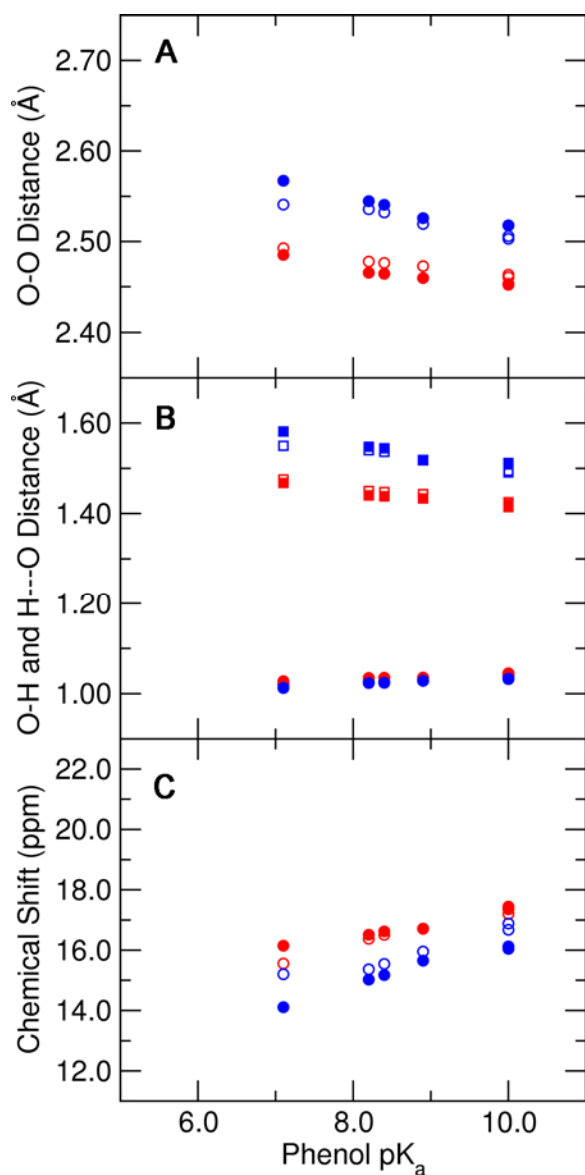
Figure S2: Comparison of the results obtained from QM/MM geometry optimizations with two different solvent configurations obtained after 500 ps (open symbols) and 1 ns (filled symbols) of solvent molecular dynamics. The following quantities are depicted as functions of the solution pK_a of the substituted phenolate: (A) the hydrogen bond O–O distances, (B) the hydrogen bond O–H distances (circles) and H---O distances (squares), and (C) the calculated NMR chemical shifts. The Tyr16-phenolate hydrogen bond is shown in red, while the Asp103-phenolate hydrogen bond is shown in blue. The ligands in these calculations were phenol, 4-fluorophenol, 3,5-difluorophenol, 3,4,5-trifluorophenol, 4-trifluoromethylphenol, and 4-nitrophenol. All calculations included Tyr16, Asp103, Asp40Asn, and the phenolate in the QM region.

Assignment of downfield peaks in ^{1}H NMR spectra of KSI•phenolate complexes

We have used the following observations to assign the far-downfield peaks observed >13 ppm in KSI•phenolate complexes to the hydrogen-bonded protons donated by Y16 and D103 to the bound phenolate. Previously published data is indicated with the appropriate citations.

1. No downfield peaks >13 ppm are observed in spectra of unliganded KSI. The 13 ppm peak observed for unliganded tKSI, which is absent in pKSI, is unchanged upon ligand binding. Data for pKSI D40N are shown above in Fig. S1. The spectrum for apo tKSI D40N (Fig. S3, below) was previously published in ref. 4.

2. Phenolate binding results in the appearance of two new downfield peaks >13 ppm (Figs. S1 & S3), as expected for the two short Y16-phenolate and D103-phenolate hydrogen bonds (O•••O distances 2.5-2.6 Å) observed in the 1.25 Å pKSI•phenolate X-ray structure (PDB 2PZV, ref. 4). Short hydrogen bond O-O distances are expected to be accompanied by elongation of the donor O-H bond that deshields the proton, resulting in a far-downfield NMR chemical shift that correlates with the hydrogen bond length (refs. 7 & 9). Spectra for tKSI D40N were previously published in ref. 4.

Figure S3: NMR Spectra of tKSI D40N•phenols
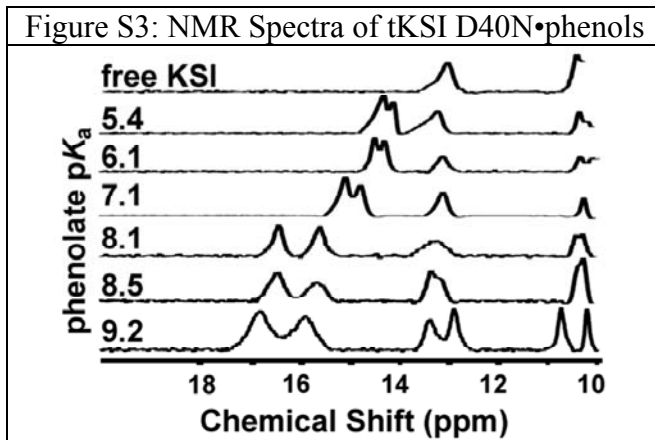
3. The two new peaks observed upon phenolate binding move progressively downfield with increasing phenolate pK_a (Figs. S1 & S3), as expected for the hydrogen bonds donated by Y16 and D103 to the phenolate oxygen.

4. Comparison of H-H NOESY spectra for the downfield peaks acquired with tKSI D40N bound to 4-nitrophenolate versus 4-nitrophenolate-d_4 (ring protons substituted with deuterons) reveals that NOE cross-peaks are detected between the downfield peaks and ring protons of the bound phenolate (Fig. S4). This result indicates that the protons giving rise to the downfield peaks are ≤5 Å from the phenolate ring, as expected for the hydroxyl protons of Y16 and D103. Data previously published in ref. 4.

Figure S4: H-H NOESY Spectra of tKSI D40N•4-nitrophenolate
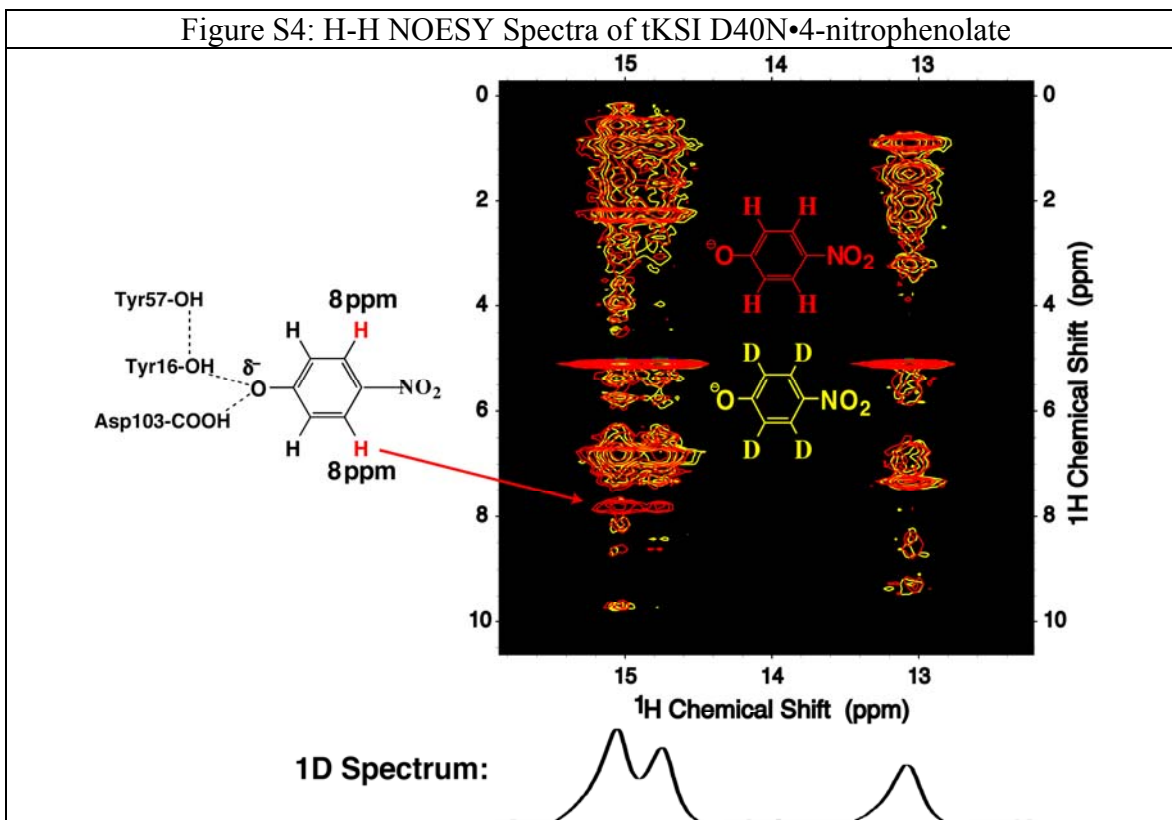
5. The D103N and Y16F mutations result in disappearance of one but not both of the downfield NMR peaks (Fig. S5), as expected for ablation of one but not both of the short hydrogen bonds formed to the bound phenolate (refs. 4 & 14).

Figure S5: NMR Spectra of 3,4-dinitrophenolate Bound to tKSI Mutants
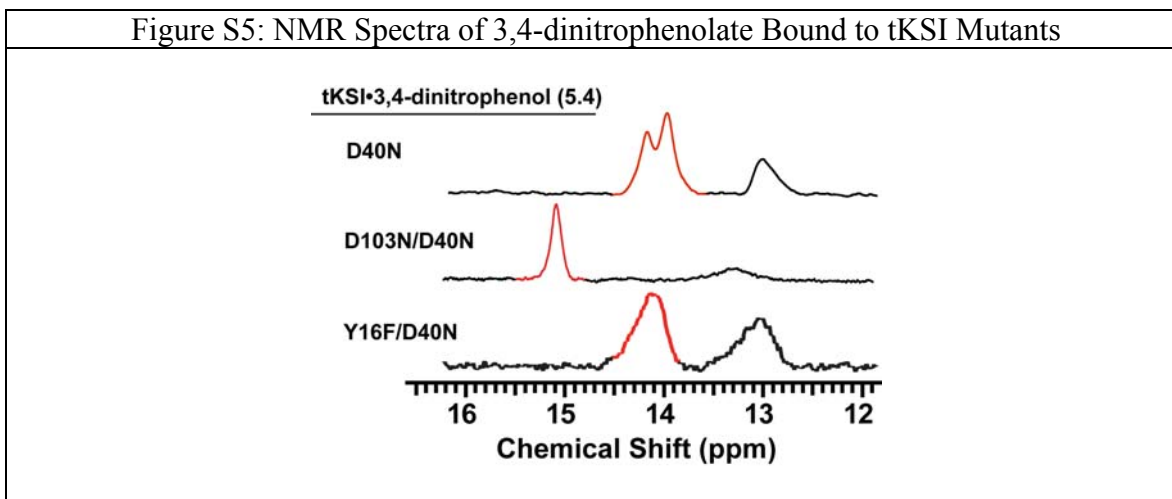
6. The Y57F mutation, which ablates the hydrogen bond donated by Y57 to the hydroxyl oxygen of Y16, results in chemical shift changes but not disappearance of the two downfield peaks (Fig. S6), as expected for retention of the two short hydrogen bonds formed by Y16 and D103 to the bound phenolate in this mutant (ref. 14). As discussed in ref. 14 and the present manuscript, the Y57F mutation is expected to weaken the

hydrogen bonding ability of Y16, resulting in an upfield shift of the hydrogen-bonded proton of Y16 and a downfield shift for the hydrogen bonded proton of D103 (relative to observed peak positions for D40N). The two hydrogen bonds observed in the Y57F mutant remain sensitive to phenolate pK_a (Fig. S6).

Figure S6: NMR Spectra for tKSI Y57F/D40N•phenols
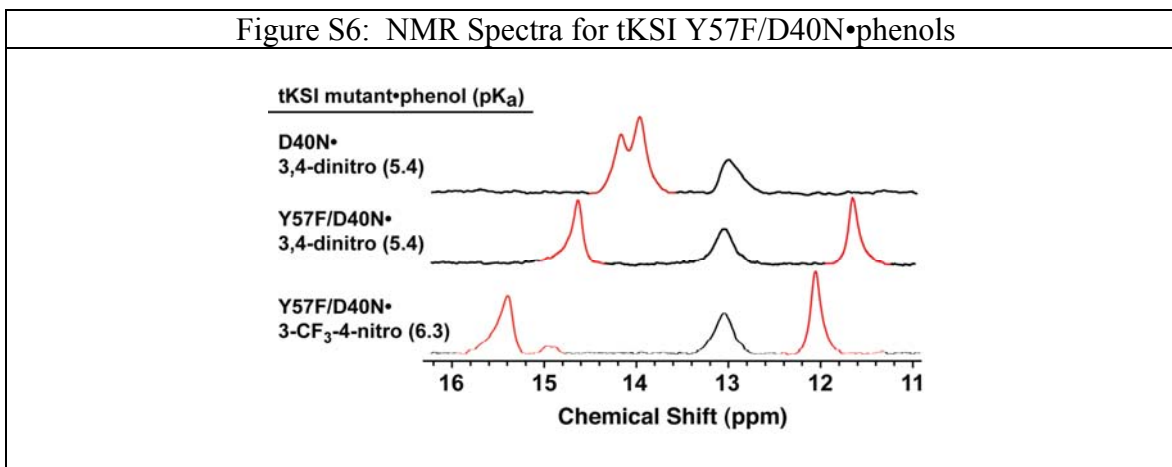
7. Solvent deuterium substitution studies indicate anti-cooperative coupling between the protons giving rise to the two downfield peaks (i.e. deuterium substitution of one proton results in a downfield shift of the other) (Fig. S7), as expected for the hydrogen-bonded protons donated by Y16 and D103 to the common acceptor oxygen of the bound phenolate (ref. 14 and background regarding anti-cooperative coupling in small molecule hydrogen bonds in Tolstoy et al. *JACS* 2004: 126, 5621). This coupling is not detected in the D103N mutant, which substantially lengthens the residue-103•phenolate hydrogen bond length from 2.6 Å to 2.9 Å (ref. 14). Data previously published in ref. 14.

Figure S7: NMR Spectra of tKSI•phenolate Complexes Upon Deuterium Substitution		
Deuterium Substitution of KSI Hydrogen Bonds	tKSI D40N•3-F-5-CF$_3$-phenol NMR Spectra	tKSI D103N/D40N•3-CF$_3$-4-nitrophenol NMR Spectra
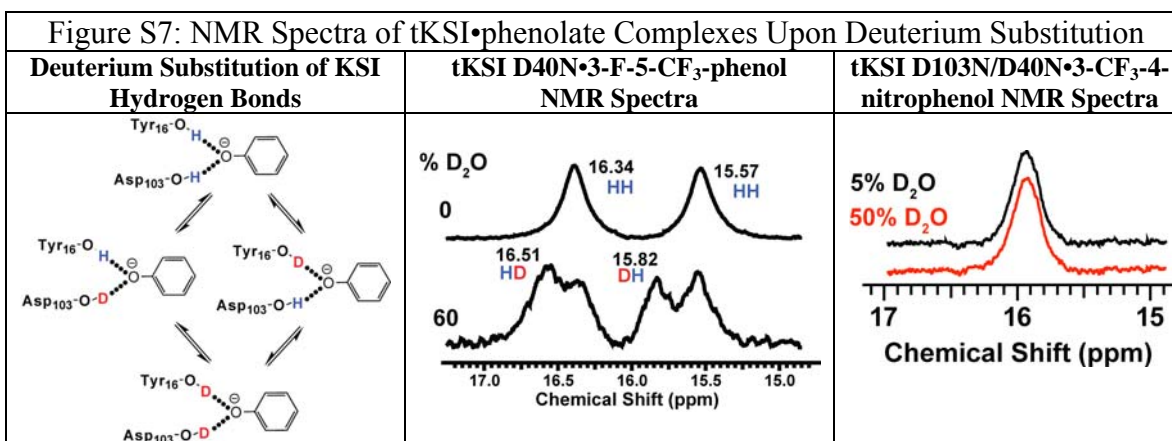
On the basis of these observations, we conclude that the downfield peaks >13 ppm observed in KSI•phenolate complexes arise from the hydrogen-bonded protons donated by Y16 and D103 to the bound phenolate. Our results, however, cannot distinguish which peak is due to which proton.

All references correspond to the main text.

Phenol	Solution pK_a
3,4-dinitrophenol	5.4
3-fluoro-4-nitrophenol	6.1
3-trifluoromethyl-4-nitrophenol	6.3
4-nitrophenol	7.1
3-nitro-4-chlorophenol	7.8
4-cyanophenol	8.0
3,5-dichlorophenol	8.1
4-acetylphenol	8.1
3,4,5-trifluorophenol	8.2
3-fluoro-5-trifluoromethylphenol	8.2
3,5-difluorophenol	8.4
3-nitrophenol	8.4
3,4-dichlorophenol	8.5
3-cyanophenol	8.6
3-trifluoromethylphenol	8.7
4-trifluoromethylphenol	8.9
3-chlorophenol	9.0
3,4-diflourophenol	9.1
3-fluorophenol	9.3
4-chlorophenol	9.4
4-fluorophenol	10.0
phenol	10.0
4-ethylphenol	10.0
4-methylphenol	10.2

Table S1: Complete list of phenols used in this work and their solution pK_a values. Solution pK_a values were obtained from Ref. (4) in the main paper and from Jencks, W.P. and Regenstein, J. (1976) In: Fasman, G.D., editor. Handbooks of biochemistry and molecular biology. Cleveland: CRC Press. pp. 305-351.